frontiers | Frontiers in Physics

TYPE Brief Research Report
PUBLISHED 05 April 2024
DOI 10.3389/fphy.2024.1386585

Check for updates

OPEN ACCESS

EDITED BY
Xiao Lin,
Zhejiang University, China

REVIEWED BY
Heyuan Guan,
Jinan University, China
Cuicui Lu,
Beijing Institute of Technology, China

*CORRESPONDENCE
Jiaxin Yu,
✉ yujiaxin@usst.edu.cn

†These authors have contributed equally to this work

RECEIVED 15 February 2024
ACCEPTED 20 March 2024
PUBLISHED 05 April 2024

CITATION
Yue K, Feng X, Yu J and Gu F (2024), Long-range air-host plasmonic propagation with subwavelength confinement.
Front. Phys. 12:1386585.
doi: 10.3389/fphy.2024.1386585

Long-range air-host plasmonic propagation with subwavelength confinement

Kun Yue†, Xialian Feng†, Jiaxin Yu* and Fuxing Gu

Laboratory of Integrated Opto-Mechanics and Electronics, Shanghai Key Laboratory of Modern Optical System, School of Optical-Electrical and Computer Engineering, University of Shanghai for Science and Technology, Shanghai, China

Confining light at a subwavelength scale is important for building ultracompact opto-electronic networks. Plasmonic waveguides are good candidate devices for this purpose. However, the oscillation of electrons relating to surface plasmon polaritons causes energy dissipation, which limits the propagation length and thus reduces the waveguide performance. Here, we design a low-loss plasmonic waveguide composed of a nanowire dimer structure on a metal substrate, in which the dominant modes are localized within the air gap between the nanowires and referred to as air-host plasmonic modes. The use of air instead of dielectric materials as the host medium can reduce ohmic loss and avoid the dispersion effect of dielectric. When the constructed nanowires have a diameter less than 100 nm, the air-host mode has subwavelength-scale confinement and a propagation length of ~100 μm, which has broad application prospects for the construction of ultracompact plasmonic devices.

KEYWORDS

plasmonic waveguide, nanowire dimer, ohmic loss reduction, light confinement, airhost plasmonic mode

1 Introduction

Plasmonic waveguides can support surface plasmon polaritons (SPPs) with a volume breaking through the optical diffraction limit [1, 2]. The strong field confinement of SPPs can enhance the interaction between light and materials [3, 4], which is beneficial for constructing energy-saving devices. Furthermore, plasmonic waveguides are small compared with traditional optical waveguides [5, 6]. Both features promise the development of ultracompact opto-electronic networks [7–11]. However, with free electrons collectively oscillating on the interface of the medium and metal, plasmonic modes suffer ohmic losses, and the energy dissipation reduces the performance of constructed devices. A figure of merit of plasmonic waveguides is a reduced ohmic loss while the field confinement of SPPs is sustained [12]. As the ohmic loss positively correlates with the dielectric index, a typical design is to insert a low-index gap layer (e.g., a MgF_2 or SiO_2 layer) between the high-index gain medium (e.g., a semiconductor nanowire) and the metal substrate (Figure 1A). The plasmonic mode then propagates along the dielectric-metal interface (in what is referred to as the dielectric-host mode) with far less loss [5, 13]. The ohmic loss can be further reduced using a medium having a lower refractive index, such as air [14], but simply replacing the dielectric with air is unfeasible as the active medium is not physically supported. Here, we design a nanowire dimer plasmonic waveguide by placing two semiconductor nanowires on a metal substrate (Figure 1B). By optimising

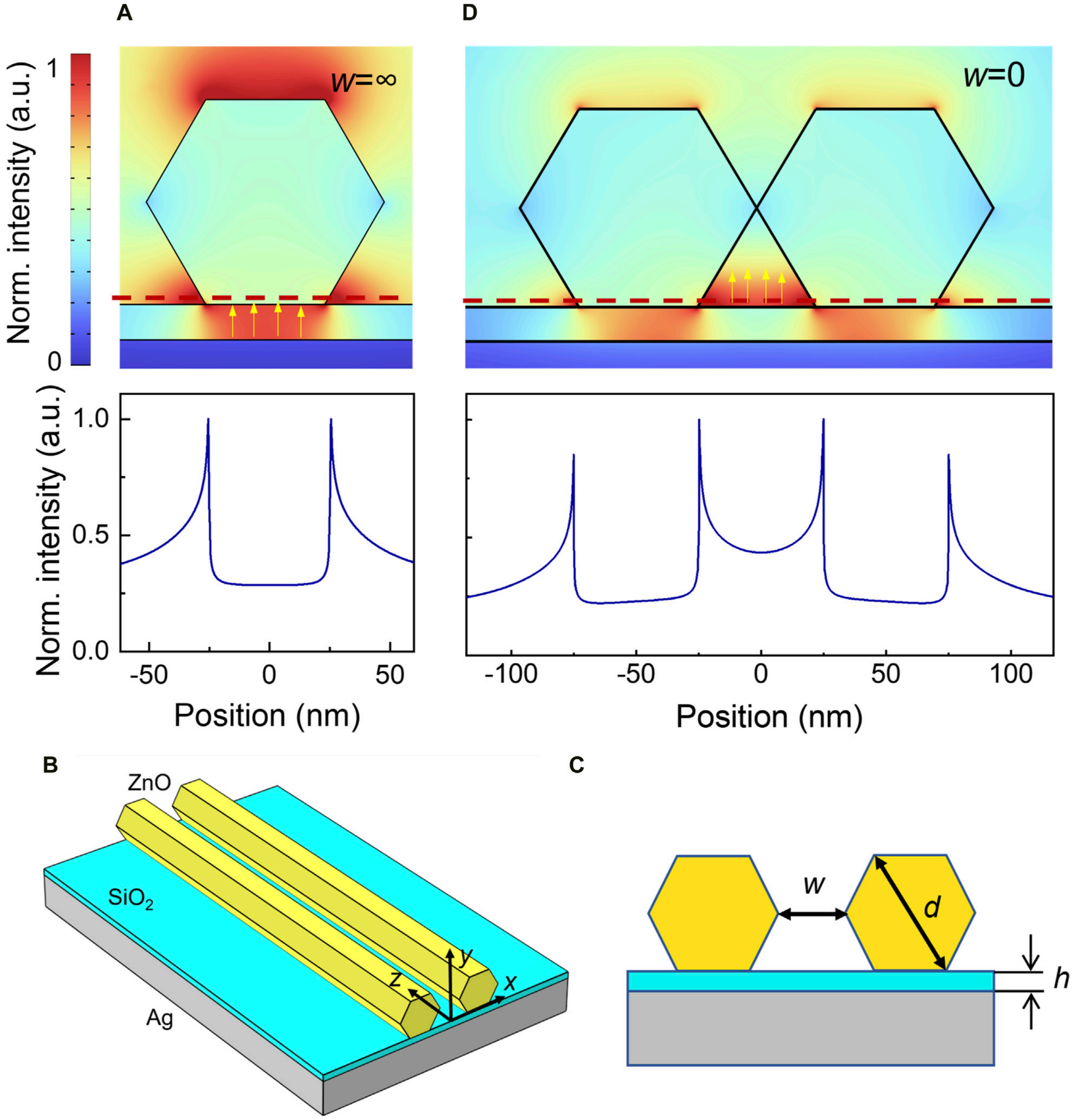

FIGURE 1
Nanowire dimer plasmonic waveguide. **(A)** Electrical field distribution of a traditional single-nanowire plasmonic waveguide, which is extracted from the resonance at around 747 nm. Three-dimensional **(B)** and cross-section **(C)** of a nanowire dimer structure. d denotes the diameter of the nanowire, w denotes the distance between two nanowires, and h denotes the thickness of the dielectric layer (SiO_2). **(D)** Field distribution of a nanowire dimer. The corresponding electric fields in **(A,D)** are extracted at 0.1 nm above the air–SiO_2 interface with d = 100 nm. The arrows in **(A,D)** show the orientation of the electric field.

parameters of the structure (i.e., the diameter and separation of the nanowires and the thickness of the dielectric layer), a low-loss propagating mode is supported in the air gap within the dimer (referred to as the air-host mode), resulting in a propagation length comparable to that of traditional single-nanowire waveguides but stronger mode confinement. Moreover, the modal field is concentrated in the air gap and is maximum at the air–dielectric interface, and the structure can thus be integrated with a microfluid chip for lasing or sensing [15]. This structure has wide prospects as a versatile platform for high-density optoelectronic devices.

2 Methods

Figure 1C presents the cross-section of a nanowire dimer plasmonic waveguide with its key parameters. The two nanowires

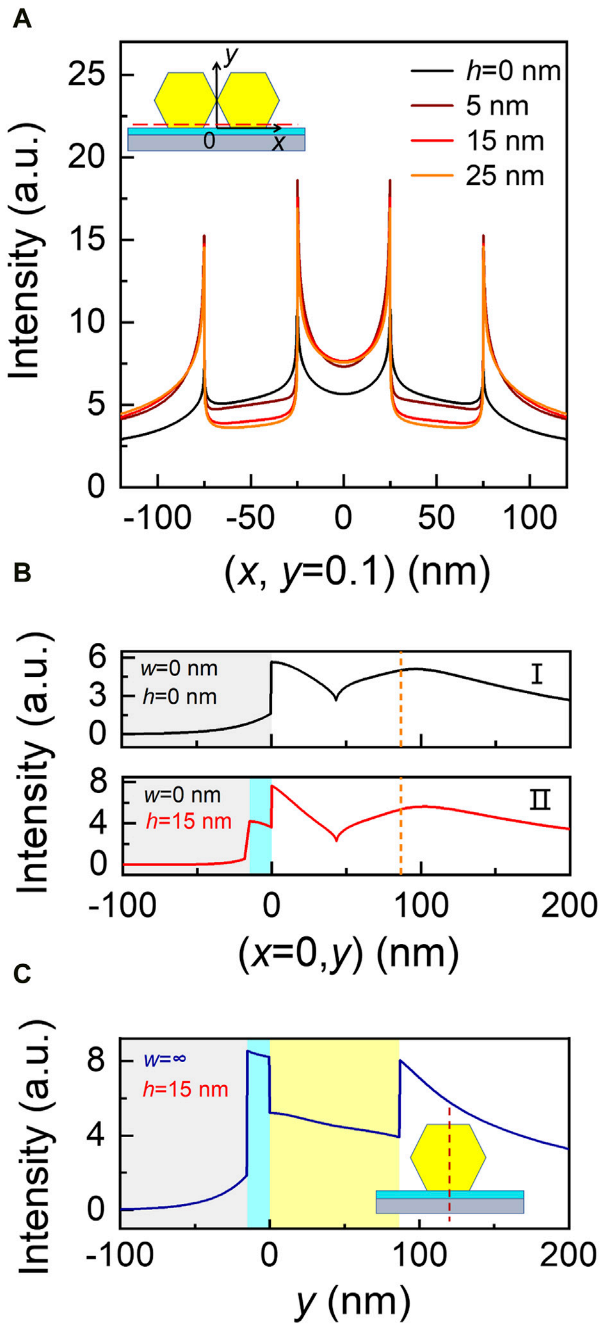

FIGURE 2
Dependence of the air-host mode on the thickness of the dielectric layer. **(A)** Dependence of the electric field at $y = 0.1$ nm (where $y = 0$ is set as the air–SiO$_2$ interface) on the layer thickness h ($w = 0$, $d = 100$ nm). When there is no dielectric layer ($h = 0$), the air-host mode is at its weakest, with an electric field comparable to the field within the nanowires, indicating a large ohmic loss from the metal substrate. An extra dielectric layer ($h \neq 0$) helps to suppress the loss to the mode field, but there is little difference in the loss as h increases from 5 to 25 nm. The independence of the air-host mode on h implies high tolerance to processing. **(B)** Dependence of the electric field at $x = 0$ (in the middle of the air gap) on the dielectric layer. The areas shaded grey and cyan are the metal and SiO$_2$ dielectric areas, respectively. The dashed lines indicate the top edges of the semiconductor nanowires. The intensity is maximal at the air–X interface (where X denotes metal for $h = 0$ or SiO$_2$ for $h \neq 0$) both with and without a SiO$_2$ layer, allowing coupling with active media settled in the air gap. **(C)** Field distribution of the dielectric-host mode at the *(Continued)*

FIGURE 2 (Continued)
middle of a single-nanowire plasmonic waveguide ($d = 100$ nm and $h = 15$ nm). The field is maximal at the metal–SiO$_2$ interface, which is comparable to the situation in **(B)**.

are made from hexagonal wurtzite-structured ZnO and have a separation w, and the metal substrate is a SiO$_2$ dielectric layer (with thickness h) deposited on bulk Ag. A simulation is performed adopting finite-difference time-domain methods for mode analysis.

3 Results and discussion

The two ZnO nanowires form an air gap between themselves and the substrate (i.e., between their feet) as illustrated in Figure 1D. For a single-nanowire waveguide (lower panel in Figure 1A), except for the strong electric field preserved in the dielectric-host mode [5, 16], there is a non-negligible field outside the nanowire. It indicates a poor light confinement especially in the case of small d (e.g., 100 nm). When two nanowires are close to one another, the fields at the enclosed foot points couple into a hybrid mode propagating in the air gap (i.e., the air-host mode), and the hybrid mode outcompetes the dielectric-host mode and dominates the propagation at small d (Figure 1D). This air-host mode has field vectors perpendicular to the substrate, and the intensity of the electric field decays evanescently with distance along the direction normal to the interface, indicating its plasmonic mode nature [12].

Inserting a dielectric layer between the metal substrate and nanowires further reduces the ohmic loss and enhances the electric field in the subwavelength local range. Therefore, we first investigate the influence of the dielectric layer on the mode fields. Figure 2A plots the distribution of mode fields along the air–SiO$_2$ interface ($y = 0.1$ nm) for different d. Compared with the structure without a SiO$_2$ layer (i.e., $h = 0$), the structure with a 5-nm-thick layer has a much stronger electric field for the air-host mode. However, in contrast with a dielectric-host mode, which is highly sensitive to h [5, 17], the air-host mode is almost unaffected by the thickness of h unless it exceeds the penetration length of the SPPs (e.g., $h > 50$ nm). The lower dependence on h is beneficial to future applications due to the better tolerance of device processing. Figure 2B shows the electric field along $x = 0$ for nanowire dimer waveguides without (I) and with a 15-nm thick dielectric layer (II). The air-host modes of the two structures have a plasmonic feature as the intensity of the electric field decreases from the bottom of the air gap. However, for the waveguide with a SiO$_2$ layer, the electric field in the air gap is much stronger than that in the SiO$_2$ layer, confirming the lower loss in air. The air-host modes can exist across a wide wavelength range, for example, from 620 nm to 1,032 nm for a dimer structure with $d = 100$ nm, $w = 0$, and $h = 15$ nm. Apart from hexagonal crystals, dimer structures composed of nanowires with other crystal types (as tetragonal crystals) also support such air-host modes. In contrast with the mode field confined in the solid dielectric layer of a traditional single-nanowire waveguide (Figure 2C), having a field confined in air

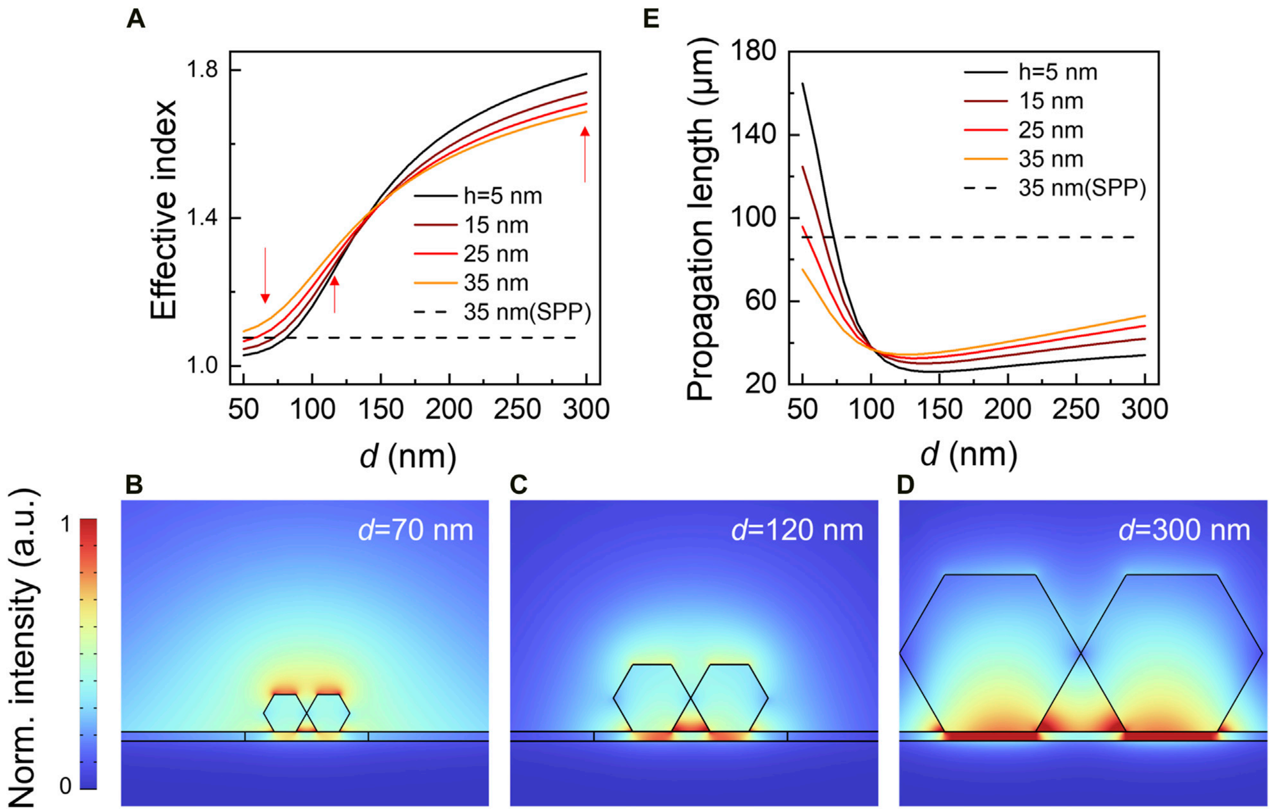

FIGURE 3
Evolution from the air-host mode to the dielectric-host mode through changes in *d* and *h*: dependence of the mode effective refractive index **(A)** and propagation length **(E)** on *d* and *h*. The dashed line provides data for SPPs supported on bare substrates without nanowires. Both the effective index and propagation length depend strongly on *d* but only slightly on *h*. **(B–D)** Electric field diagrams for $d = 70$, 120, and 300 nm ($h = 15$ nm, $w = 0$ nm), showing the evolution of dominance from the air-host mode to dielectric-host mode.

makes the waveguide easier to functionalise and modulate for applications.

To gain a deeper understanding of the air-host mode, we analyse the dependence of the effective refractive index (n_{eff}) on d and h, where $n_{eff} = \beta/k_0$. Here, β is the propagation constant of the plasmonic modes and k_0 is the vacuum wavenumber. Figure 3A shows that the real part of n_{eff} for $h = 5$ nm ($w = 0$) increases monotonously from ~1 to ~1.8 as the nanowire diameter increases from 50 to 300 nm, revealing an evolution from air-host modes to dielectric-host modes. Specifically, for nanowires with a small diameter (i.e., 50 nm < d < 100 nm), the waveguide is dominated by an air-host mode which represents a low effective index compared to the material index of SiO_2 (1.453). It can be visualized from the electric field distribution in Figure 3B. The field leaked outside the nanowires strongly couple with each other and resonantly intensify at the air gap [18, 19], whereas the energy density in the SiO_2 dielectric layer is negligible. A larger diameter of the nanowires induces competition between the air-host mode and dielectric-host mode given the reduced near-field coupling effect between the two nanowires. As shown in Figure 3C, the field is a superposition of the two types of modes, and the effective index approaches the index of SiO_2 with the increase of the diameter [20]. When the diameter is large enough (i.e., 150 nm < d < 300 nm), the dielectric-host mode becomes dominant, representing as a strongest field intensity in the SiO_2 layer under the individual nanowires, and the effective index exceeds the index of SiO_2 (Figure 3D).

The ohmic losses corresponding to the two modes are quantified by the imaginary part of the effective index, Im$\{n_{eff}\}$, which further determines the propagation length (L_P). L_P can be calculated by $L_P = \lambda_0/\left(4\pi \mathrm{Im}\left\{n_{eff}\right\}\right)$, which is defined as the distance travelled in space before the energy density of the mode decays to its initial value $1/e$ (λ_0 is the vacuum wavelength). As shown in Figure 3E, when the air-host mode dominates, the propagation length L_P can be tens to more than one hundred microns, comparable to the length scale of optimised single-nanowire waveguides. When the dimer structure is dominated by a superposition of the air-host and dielectric-host modes, the plot of L_P has an inflection due to the mode competition, such that there is a minimal value of L_P. When the waveguide is dominated by the dielectric-host mode, L_P increases with d. However, the available L_P is much shorter for the dielectric-host mode than for the air-host mode (no more than 50 μm), indicating the superior performance of the latter mode. Considering that L_P is longer for smaller nanowires, the nanowire dimer waveguide is conducive to device integration.

Light–matter interactions are of great interest owing to their potential applications in such as lasing and sensing [21, 22]. The basic idea of using an optical waveguide to enhance such interaction is to confine light in a small spatial region and to increase the

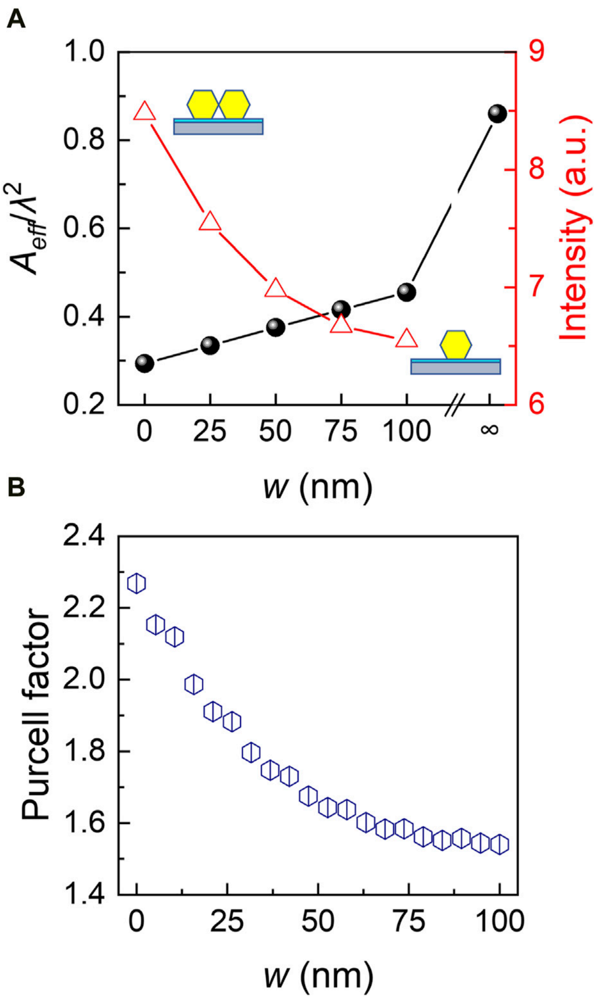

FIGURE 4
Mode confinement and Purcell effect of a nanowire-dimer waveguide. **(A)** Variations in the normalised effective mode area and electric field intensity with *w*. The electric field intensity is extracted from the central axis of the air gap, 0.1 nm above the air–SiO_2 interface. The nanowire-dimer waveguide with $w = 0$ has the most confined field, the intensity of which is only 1/3 of that of a single-nanowire waveguide ($w = \infty$). **(B)** Variation in the Purcell factor with *w*. The strongest enhancement of spontaneous emission is achieved using a nanowire-dimer waveguide with $w = 0$.

light–matter overlap. The confinement can be quantified by the effective mode area (A_{eff}) [13], expressed as

$$A_{eff} = \iint_{-\infty}^{\infty} W(\mathbf{r})\mathrm{d}^2\mathbf{r} \Big/ \max\{W(\mathbf{r})\} \tag{1}$$

Here, the energy density $W(\mathrm{r})$ is defined as

$$W(\mathbf{r}) = \frac{1}{2}\mathrm{Re}\left\{\frac{\mathrm{d}[\omega\varepsilon(\mathbf{r})]}{\mathrm{d}\omega}\right\}|\mathbf{E}(\mathbf{r})|^2 + \frac{1}{2}\mu_0|\mathbf{H}(\mathbf{r})|^2 \tag{2}$$

where ω is the mode resonance frequency, $\varepsilon(r)$ is the complex relative permittivity, and μ_0 is the vacuum permeability. A_{eff} calculated from Eqs (1, 2) is then normalised by the square of the wavelength (i.e., we take $A_{eff}/{\lambda_0}^2$) [23]. The dependence of normalised A_{eff} on w represents the effect of nanowire coupling on the confinement of the air-host mode (black solid circles in Figure 4A, $d = 100$ nm and $h = 15$ nm). When w is much larger than the wavelength scale, the coupling between nanowires is negligible and the structure works as a traditional single-nanowire waveguide, which has a mode field of ~$0.86\lambda^2$. As w decreases, the nanowire coupling strengthens, and the mode is more confined to the air gap. This is seen as a gradual decrease in the normalised mode area (black circles) and an enhanced electromagnetic field (red triangles). When the nanowires are in contact with each other ($w = 0$), the mode area reaches a minimal value of ~$0.29\lambda^2$, approximately 3 times smaller than that of a single-nanowire structure ($w = \infty$) and nearly one order smaller than that of planar SPPs on the same substrate.

As the maximum field appears in the air gap (namely, at the air–SiO_2 interface) rather than in a bulk medium, an optimal light–matter interaction can be easily achieved by placing active materials at the interface [21, 24], which is meaningful for applications. For example, by attaching a monolayer semiconductor (such as transition metal chalcogenides) at the interface, a perfect overlap between the two-dimensional gain medium and mode is achieved. The modal gain is thus maximised for plasmonic lasing [22, 25]. The waveguide modification of the spontaneous emission can be quantified using the Purcell factor (F_P) [26]. The spontaneous emission of excitons in the monolayers (~1.0 nm in thickness) is mimicked by setting electric dipole sources in the middle of the air gap and 0.1 nm above the interface, and the enhancement of the recombination rate can be simulated by the change in the lifetime. As shown in Figure 4B, F_P increases as the nanowire coupling strengthens and has a maximal value of 2.3 at $w = 0$. As the intensity at the foot points can be even stronger, the actual F_P can be even higher. Due to the strong mode confinement and Purcell effect, the nanowire dimer structure has good potential for ultracompact plasmonic active devices using atomically thick active media [27, 28].

4 Conclusion

In summary, we proposed a plasmonic waveguide composed of a nanowire dimer on a metal substrate. The air-host mode supported by such a nanowire dimer structure has low ohmic loss and thus a long propagation length. Compared with a single nanowire plasmonic waveguide, the nanowire dimer waveguide has stronger mode confinement, a high Purcell factor at the air–dielectric interface, and thus more intense light–matter interaction. In addition, the properties of the waveguides have higher tolerance to the processing of the dielectric layer. As the dominant mode of propagation is in an air gap instead of a dielectric solid, nanowire dimer plasmonic waveguides are a more versatile platform for constructing functional integrated devices.

Data availability statement

The original contributions presented in the study are included in the article, further inquiries can be directed to the corresponding author.

Author contributions

KY: Formal Analysis, Investigation, Writing–original draft. XF: Formal Analysis, Investigation, Writing–review and editing. JY: Conceptualization, Funding acquisition, Supervision, Writing–original draft, Writing–review and editing. FG: Funding acquisition, Writing–review and editing.

Funding

The author(s) declare that financial support was received for the research, authorship, and/or publication of this article. This work was supported by the National Natural Science Foundation of China (NSFC) (Grant Nos 12074259, 62075131, and 62122054).

Conflict of interest

The authors declare that the research was conducted in the absence of any commercial or financial relationships that could be construed as a potential conflict of interest.

Publisher's note

References

1. Zhu W, Xu T, Wang H, Zhang C, Deotare PB, Agrawal A, et al. Surface plasmon polariton laser based on a metallic trench Fabry-Perot resonator. *Sci Adv* (2017) 3: e1700909. doi:10.1126/sciadv.1700909

2. Zhang Q, Li G, Liu X, Qian F, Li Y, Sum TC, et al. A room temperature low-threshold ultraviolet plasmonic nanolaser. *Nat Commun* (2014) 5:4953. doi:10.1038/ncomms5953

3. Ning CZ. Semiconductor nanolasers and the size-energy-efficiency challenge: a review. *Adv Photon* (2019) 1:1. doi:10.1117/1.AP.1.1.014002

4. Ma RM, Oulton RF, Sorger VJ, Bartal G, Zhang X. Room-temperature sub-diffraction-limited plasmon laser by total internal reflection. *Nat Mater* (2011) 10:110–3. doi:10.1038/nmat2919

5. Oulton RF, Sorger VJ, Zentgraf T, Ma RM, Gladden C, Dai L, et al. Plasmon lasers at deep subwavelength scale. *Nature* (2009) 461:629–32. doi:10.1038/nature08364

6. Tao T, Zhi T, Liu B, Dai J, Zhuang Z, Xie Z, et al. Manipulable and hybridized, ultralow-threshold lasing in a plasmonic laser using elliptical inGaN/GaN nanorods. *Adv Funct Mater* (2017) 27:1703198. doi:10.1002/adfm.201703198

7. Noginov MA, Zhu G, Belgrave AM, Bakker R, Shalaev VM, Narimanov EE, et al. Demonstration of a spaser-based nanolaser. *Nature* (2009) 460:1110–2. doi:10.1038/nature08318

8. Toanen V, Symonds C, Benoit JM, Gassenq A, Lemaitre A, Bellessa J. Room-Temperature lasing in a low-loss tamm plasmon cavity. *ACS Photon* (2020) 7:2952–7. doi:10.1021/acsphotonics.0c00781

9. Suh JY, Kim CH, Zhou W, Huntington MD, Co DT, Wasielewski MR, et al. Plasmonic bowtie nanolaser arrays. *Nano Lett* (2012) 12:5769–74. doi:10.1021/nl303086r

10. Liu Y, Ma Y. One-dimensional plasmonic sensors. *Front Phys* (2020) 8:312. doi:10.3389/fphy.2020.00312

11. Linghu S, Gu Z, Lu J, Fang W, Yang Z, Yu H, et al. Plasmon-driven nanowire actuators for on-chip manipulation. *Nat Commun* (2021) 12:385. doi:10.1038/s41467-020-20683-2

12. De Leon I, Berini P. Amplification of long-range surface plasmons by a dipolar gain medium. *Nat Photon* (2010) 4:382–7. doi:10.1038/nphoton.2010.37

13. Wang Y, Wang S, Cai M, Liu H. A long propagation distance hybrid triangular prism waveguide for ultradeep subwavelength confinement. *IEEE Sens J* (2019) 19:11159–66. doi:10.1109/JSEN.2019.2935750

14. Hentschel M, Koshelev K, Sterl F, Both S, Karst J, Shamsafar L, et al. Dielectric Mie voids: confining light in air. *Light Sci Appl* (2023) 12:3. doi:10.1038/s41377-022-01015-z

15. Anker JN, Hall WP, Lyandres O, Shah NC, Zhao J, Van Duyne RP. Biosensing with plasmonic nanosensors. *Nat Mater* (2008) 7:442–53. doi:10.1038/nmat2162

16. Liu X, Zhang Q, Yip JN, Xiong Q, Sum TC. Wavelength tunable single nanowire lasers based on surface plasmon polariton enhanced Burstein-Moss effect. *Nano Lett* (2013) 13:5336–43. doi:10.1021/nl402836x

17. Li Z, Bao K, Fang Y, Guan Z, Halas NJ, Nordlander P, et al. Effect of a proximal substrate on plasmon propagation in silver nanowires. *Phys Rev B Condens Matter Mater Phys* (2010) 82:241402. doi:10.1103/PhysRevB.82.241402

18. Wuestner S, Hamm JM, Pusch A, Hess O. Plasmonic leaky-mode lasing in active semiconductor nanowires. *Laser Photon Rev* (2015) 9:256–62. doi:10.1002/lpor.201400231

19. Chen Y, Gregersen N, Nielsen TR, Mørk J, Lodahl P. Spontaneous decay of a single quantum dot coupled to a metallic slot waveguide in the presence of leaky plasmonic modes. *Opt Express* (2010) 18:12489–98. doi:10.1364/oe.18.012489

20. Bian Y, Gong Q. Tuning the hybridization of plasmonic and coupled dielectric nanowire modes for high-performance optical waveguiding at sub-diffraction-limited scale. *Sci Rep* (2014) 4:6617. doi:10.1038/srep06617

21. De Torres J, Ferrand P, Colas Des Francs G, Wenger J. Coupling emitters and silver nanowires to achieve long-range plasmon-mediated fluorescence energy transfer. *ACS Nano* (2016) 10:3968–76. doi:10.1021/acsnano.6b00287

22. Liu X, Galfsky T, Sun Z, Xia F, Lin EC, Lee YH, et al. Strong light-matter coupling in two-dimensional atomic crystals. *Nat Photon* (2014) 9:30–4. doi:10.1038/nphoton.2014.304

23. Oulton RF, Sorger VJ, Genov DA, Pile DFP, Zhang X. A hybrid plasmonic waveguide for subwavelength confinement and long-range propagation. *Nat Photon* (2008) 2:496–500. doi:10.1038/nphoton.2008.131

24. Sidiropoulos TPH, Röder R, Geburt S, Hess O, Maier SA, Ronning C, et al. Ultrafast plasmonic nanowire lasers near the surface plasmon frequency. *Nat Phys* (2014) 10:870–6. doi:10.1038/nphys3103

25. Paik EY, Zhang L, Burg GW, Gogna R, Tutuc E, Deng H. Interlayer exciton laser of extended spatial coherence in atomically thin heterostructures. *Nature* (2019) 576:80–4. doi:10.1038/s41586-019-1779-x

26. Barthes J, Colas DFG, Bouhelier A, Weeber JC, Dereux A. Purcell factor for a point-like dipolar emitter coupled to a two-dimensional plasmonic waveguide. *Phys Rev B Condens Matter Mater Phys* (2011) 84:073403. doi:10.1103/PhysRevB.84.073403

27. Liao F, Yu J, Gu Z, Yang Z, Hasan T, Linghu S, et al. Enhancing monolayer photoluminescence on optical micro/nanofibers for low-threshold lasing. *Sci Adv* (2019) 5:eaax7398. doi:10.1126/sciadv.aax7398

28. Yu JX, Xing S, Dai GY, Ling-Hu SY, Gu FX. Direct-bandgap bilayer WSe2/microsphere monolithic cavity for low-threshold lasing. *Adv Mater* (2022) 34:2106502. doi:10.1002/adma.202106502